The effect of pore structure and gas pressure upon the transport properties of coal: a laboratory and modeling study.
1. Isotherms and pore volume distributions

C.R. Clarkson[a,*], R.M. Bustin[b]

[a]*Burlington Resources, San Juan Division, 3535 E. 30th St. 87402-8801, P.O. Box 4289, Farmington, NM, 87499-4289, USA*
[b]*Department of Earth and Ocean Sciences, The University of British Columbia, 6339 Stores Road, Vancouver, BC, V6T 1Z4, Canada*

Abstract

The effect of coal composition upon pore structure and adsorption characteristics of four bituminous coals of the Cretaceous Gates Formation coal is investigated. All the coals have multi-modal pore volume distributions as determined from low-pressure (<127 kPa) nitrogen adsorption at 77 K, carbon dioxide adsorption at 273 K, and high-pressure (up to 200 MPa) mercury porosimetry. The individual lithotypes, however, differ in their pore volume distributions and adsorption characteristics. The dull coals (high inertinite, high ash content) have a greater percentage of mesoporosity and less microporosity than bright or banded bright coals (high vitrinite, low ash content) of the same rank. In addition, one banded bright coal has a greater amount of macroporosity than the other coals.

High-pressure (up to ~8 MPa) methane isotherms determined on dried and moisture-equilibrated coals, and carbon dioxide isotherms (up to ~ 5 MPa) determined on dried coal at 303 K, show that bright coals tend to adsorb more gas than dull coals. The Dubinin–Astakhov equation provides a better fit to coal gas isotherm data, particularly for carbon dioxide, than the conventionally used Langmuir equation. There is a linear correlation between high-pressure methane and carbon dioxide Langmuir volumes and Dubinin–Radushkevich micropore volumes, indicating that micropore volume is a primary control upon high-pressure gas adsorption for the Gates coals. © 1999 Elsevier Science Ltd. All rights reserved.

Keywords: Coal; Isotherms; Pore volume distributions

1. Introduction

Knowledge of coal adsorption characteristics and pore structure is useful for a variety of different applications including the prediction of coal gas outbursts in coal mines, the economic recovery of natural gas from coal seams, and characterization of coals as a pre-cursor for activated carbons. Recent studies [1–4] have shown that pore structure has an important effect upon methane gas transport through the coal matrix.

Coal is a complex polymeric material with a complicated porous structure that is difficult to classify. Previous studies [5–8] have used traditional gas adsorption methods and helium and mercury porosimetry in an attempt to determine the pore volume distribution and total porosity of coal. Gan et al. [5] demonstrated that pore volume distribution is dependent upon the rank of coal. In the Gan et al. study,

total pore volumes were divided into: micropores (0.4–1.2 nm), transitional pores (1.2–30 nm), and macropores (30–2960 nm). The current study utilizes the IUPAC classification [9]. Lower-rank coals (carbon content < 75%) contain mainly macropores, coals in the 76–84% fixed carbon content range contain mainly micro- and transitional pores, and high rank coals (carbon content > 84%) contain mainly micropores.

Some studies have focussed upon determining the microporosity and micropore distributions of coal using carbon dioxide gas adsorption [10–13]. The proportion of microporosity in coal samples is believed to be an important controlling factor upon the adsorption of methane. Carbon dioxide isotherms, usually measured at 273 and 298 K, are useful in determining coal micropore volumes and surface areas, because carbon dioxide gas is able to access the finest porosity at these temperatures. Nitrogen gas at 77 K is generally not considered to have access to the finest microporosity of coal owing to the activated diffusion effect and/or pore shrinkage [14] at low temperatures. Possible complications arising from the use of carbon dioxide

* Corresponding author. Tel: + 1-505-326-9729; fax: + 1-505-599-4017.
E-mail address: cclarkson@br-inc.com (C.R. Clarkson)

include specific interaction between coal and carbon dioxide due to the large quadrupole moment of carbon dioxide, and coal swelling during adsorption.

Confusion about the effect of coal type upon gas adsorption capacity of coal still exists. Lamberson and Bustin [15], who studied methane adsorption upon moisture-equilibrated coals of varying petrographic composition, have shown that methane gas adsorption, on a mineral matter-free basis, generally increases with an increase in the vitrinite content. Levine et al. [16], have shown that the methane adsorption capacity of dry coal, determined using the gravimetric method, is greater for vitrinite concentrates than for inertinite concentrates. Bright coals of the Bowen Basin, Australia, were shown to have a greater methane adsorption capacity than dull coals of the same rank [16] and methane capacity was positively correlated with vitrinite content for moisture-equilibrated coals of the Sydney Basin [17]. Ettinger et al. [18], however, reported that gas yields increase with fusain content. Faiz et al. [8] noted that dry, ash-free Langmuir volumes show a slight negative correlation with inertinite content, but stated that the correlation may be masked by rank variations between samples. It is generally accepted that gas adsorption decreases with an increase in the ash content in coal samples.

The purpose of the current study is to determine the (equilibrium) adsorption/desorption properties and pore volume distributions of four lithotypes from the Cretaceous Gates Formation of Northeast B.C. in order to assess the effect of these properties upon adsorption rate behavior (the subject of Part 2). The current study utilizes an integrated approach to the characterization of pore volume distribution for coals of varying (organic and mineral) composition, similar to the approach used by Gan et al. [5] and Unsworth et al. [7], to determine the effect of pore volume distribution upon high-pressure adsorption methane and carbon dioxide isotherms. Ambiguities regarding the effect of coal type and pore volume distribution upon high-pressure methane and carbon dioxide will be addressed. The results of this study will be incorporated into a new numerical matrix gas transport model, developed in Part 2. Additionally, these results will lead to a better understanding of the factors controlling the release of methane or coalbed gas from the coal matrix, and hence will be applicable to the prediction of gas transport and outbursting phenomena.

2. Methods

2.1. Sample location and preparation

Four medium-volatile bituminous coal lithotype samples from the Lower Cretaceous Gates Formation of northeastern British Columbia were chosen for this study. The samples were crushed by hand (stage crushed) to pass through a 4 mesh (4.75 mm) sieve and four sub-samples were obtained. A -4 mesh fraction was retained and the other sub-samples

were crushed to pass through an 8 (2.38 mm), 20 (0.841 mm), and 60 (0.250 mm) mesh sieve. Only the -4 and -60 mesh fractions were used for isotherm analysis. The -60 mesh fraction was also utilized for proximate (ash and moisture) and petrographic analysis. Petrographic analysis was performed using manual point counts on polished pellets [19].

A sieve analysis was performed on the -4 mesh coals in order to determine the mean particle size to be used in adsorption rate analysis (Part 2). For all coals, greater than 90 wt.% was collected between sieve size diameters 2.38 and 4.75 mm. Two estimates of mean particle size were used: the harmonic mean [20], and the arithmetic average of the upper and lower limits of the most frequent fraction. Using the latter estimate, the mean particle radius for all coals is 1.84 mm.

2.2. Low-pressure isotherm analysis

Low-pressure (<0.127 MPa) isotherm analyses were performed on a Micromeritics ASAP 2010® volumetric gas adsorption apparatus. Carbon dioxide equilibrium isotherms were collected at 273 K (ice/water bath) for -4 and -60 mesh fractions of the lithotype samples. Samples were evacuated at 100°C for at least 12 h on the apparatus until a pressure of <0.25 Pa was reached. Other details of isotherm analysis are given elsewhere [13]. The Dubinin–Radushkevich (D–R) equation [21] was used to obtain micropore volumes. Coefficients of variation for D–R micropore volumes are less than 5% based upon repeat analysis of -60 and -4 mesh splits of the coals.

Nitrogen (77 K) adsorption/desorption isotherms were collected on the -60 mesh splits. Difficulty in achieving equilibrium was encountered with the -4 mesh splits, likely due to the extremely slow diffusion rates of nitrogen gas at 77 K, therefore the coarser particles were not used for nitrogen adsorption work. The BET equation [22] was used to obtain surface areas from the nitrogen isotherm data. BET surface areas were calculated from data in the 0.06–0.2 relative pressure range. Barrett, Joyner, Halenda (BJH) theory [23] was used to obtain mesopore (pore diameter 2–50 nm) distributions from the desorption branch of the nitrogen isotherm. BJH cumulative and differential pore volume distributions were determined for the desorption branch of the isotherm. Coefficients of variation for mesopore volumes, determined from repeat runs of several samples, were less than 9%.

2.3. High-pressure isotherm analysis

dioxide isotherms were determined using a sample that overnight and then evacuated at isotherm temperature for 24 h. In addition, methane isotherms were determined

Table 1
Maceral composition (volume %, mmf), moisture (weight %, air-dry), and ash yields (weight %, dry-basis)

Sample	Structured vitrinite[a]	Desmocollinite	Semifusinite	Fusinite	Other inertinite[b]	Liptinite	Moisture (%)	Ash (%)
C3-2	75	23	1	1	–	–	0.5	12.7
B2-11	29	30	33	5	3	–	0.5	3.3
D3-3	20	30	23	–	27	–	1.2	46.7
B2-10	13	28	49	3	6	1	0.3	29.7

[a] Includes telocollinite and telinite.
[b] Includes macrinite and inertodetrinite.

coals. Equilibrium moisture (at ▮▮▮▮▮▮) was achieved using a procedure similar to that described by Levy et al. [25].

Equilibrium at each isotherm point is assumed to have been reached if the pressure reading was stable ($\Delta P = 0.000$ MPa) for about 7 h (400 min) for the -4 mesh coals. Much less time was required for equilibrium for -60 mesh coals. For the adsorption isotherm, a program, as described in Levy et al. [26], was used to automate data collection. Volume adsorbed calculations are performed according to the procedure described by Levy et al. [26].

The isotherm equation used to model equilibrium high-pressure gas adsorption data is that proposed by Langmuir [27]. The equation may be expressed for plotting purposes as:

$$\frac{P}{V} = \frac{P}{V_L} + \frac{P_L}{V_L}.$$ (1)

A linear regression is performed for P/V vs. P plots to obtain the Langmuir constants.

The Langmuir equation was used to model equilibrium isotherm data for adsorption rate modeling (Part 2). The coefficient of variation of the Langmuir volume (V_L) and Langmuir pressure (P_L), determined from repeat measurements of methane isotherms on dried -4 and -60 mesh coals, were less than 6 and 17%, respectively.

Alternatively, the Dubinin–Astakhov equation may be used to model high-pressure adsorption data [28]. The D–A equation, written for plotting purposes, is:

$$\log W = \log W_o - D(\log P_o/P)^n$$ (2)

where W the amount of gas adsorbed, W_0 the micropore volume, P_0 the saturation vapor pressure, and n is the Astakhov exponent. Procedures for determining pseudo-saturation vapor pressure above critical temperature are described elsewhere [28]. The three parameters W_0, D, and n were optimized using a least squares routine coupled with a multiparameter optimization algorithm in MATLAB®.

2.4. He and Hg porosimetry

Helium densities were determined using helium expansion at 30°C on the high-pressure volumetric adsorption apparatus. A split of about 2 g was taken from the isotherm samples (-4 mesh) and used for mercury porosimetry analysis, on a Micromeritics Poresizer 9320®. The samples were evacuated at 110°C for at least 3 h prior to analysis and then evacuated on the instrument for 15 h until a stable pressure was reached.

As mentioned by Gan et al. [5], there is some uncertainty about what is the minimum pressure required to fill inter-particle voids when powders are used in mercury density
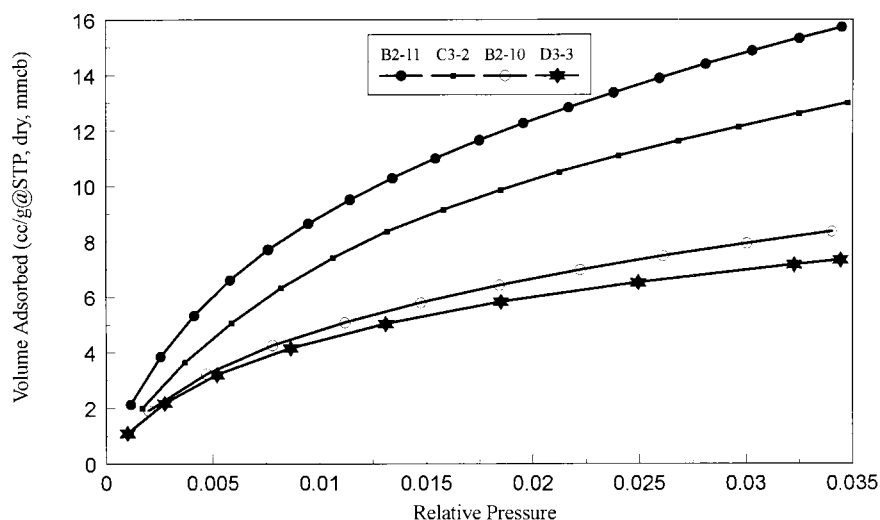

Fig. 1. 273 K low-pressure carbon dioxide isotherms obtained from -60 mesh splits.

Table 2
Surface areas and micro/mesopore volumes of coals

Sample	BET s.a. (m^2/g, dry, mmcb)	BET s.a. (m^2/g, daf)	D–R mic.v.[a] (cm^3/g, dry, mmcb)	D–R mic.v.[a] (cm^3/g, daf)	D–R mic.v.[b] (cm^3/g, dry, mmcb)	BJH mes. v. (cm^3/g, dry, mmcb)	BJH mes. v. (cm^3/g, daf)
C3-2	0.7 (1)	0.8	.049	.057	N/A	0.001 (1)	0.001
B2-11	0.7 (3)	0.7	.055	.057	.054	0.001 (3)	0.001
D3-3	2.7 (3)	5.0	.025	.046	.027	0.004 (3)	0.008
B2-10	2.2 (1)	3.1	.028	.040	.027	0.006 (1)	0.008

[a] Determined for -60 mesh coal.
[b] Determined for -4 mesh coal.

determination. For a -20 mesh particle size, a pressure of about 0.41 MPa was required to fill the interparticle void volume [29]. The pressure required to fill the interparticle void space may be approximated by obtaining mercury intrusion volumes with pressure for nonporous materials of the same particle size (such as glass beads) [5]. In the current study, the -4 mesh coal particle density was determined using the following procedure: a known mass of mercury was injected at near ambient pressures into a penetrometer of known volume containing the coal of known mass; the volume of mercury injected was determined from its mass and the density of mercury at the analysis temperature; the difference between the injected mercury volume and the calibrated penetrometer volume was taken

as the total particle volume of the coals; the coal (particle) density was determined from the coal mass and total particle volume. In this analysis, the volume of voids between particles is assumed to be filled at near ambient pressures. Negligible amounts of mercury were intruded below 0.207 MPa (~30 psia) for all samples therefore indicating that the interparticle void space had probably been filled at pressures <0.207 MPa. The coefficient of variation for Hg density measurements is less than 2% based upon repeated analysis of different (-4 mesh) sample splits.

Mercury intrusion data was collected up to a maximum pressure of about 200 MPa (30 000 psia). A contact angle of 130° [5] and surface tension of 485 dyn/cm was used in the
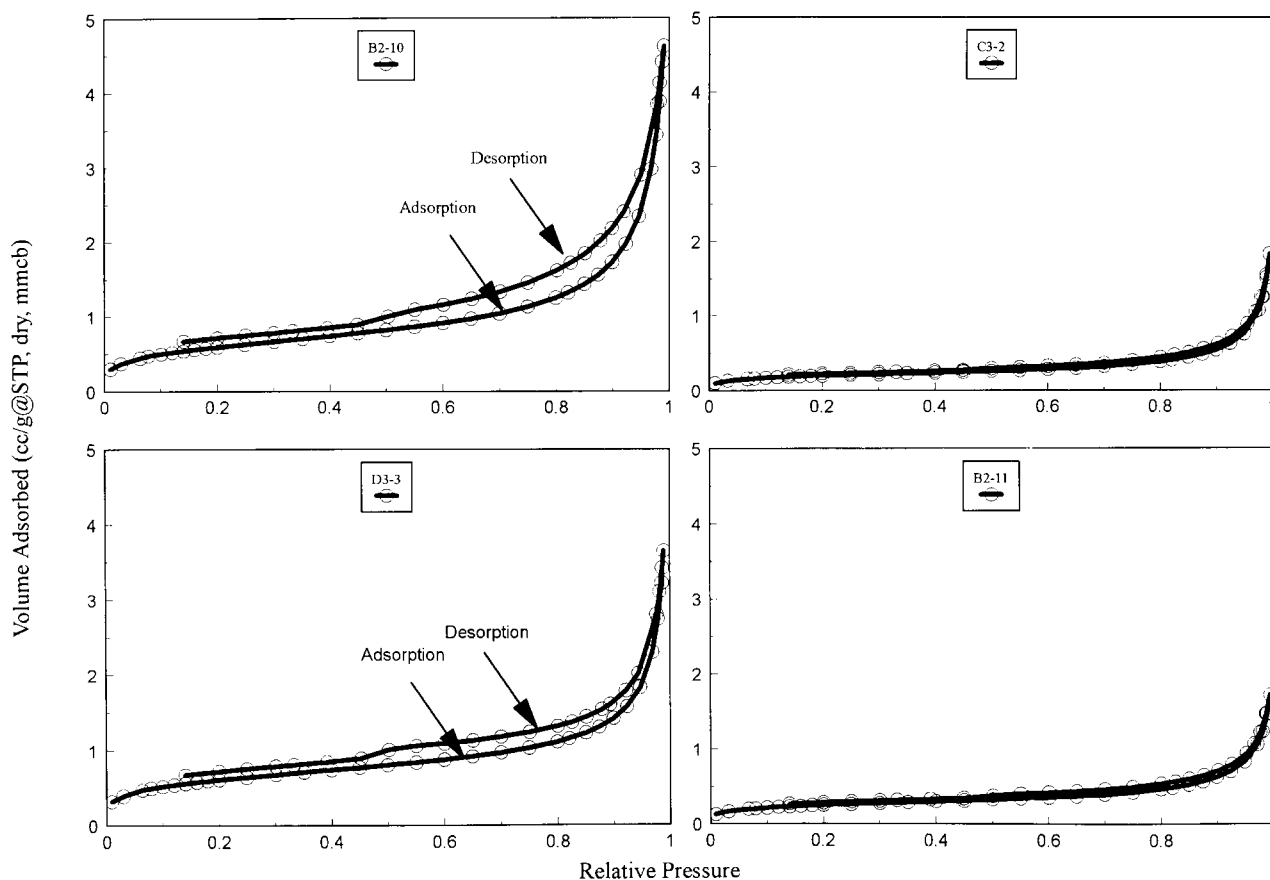

Fig. 2. 77 K low-pressure nitrogen isotherms obtained from -60 mesh splits.
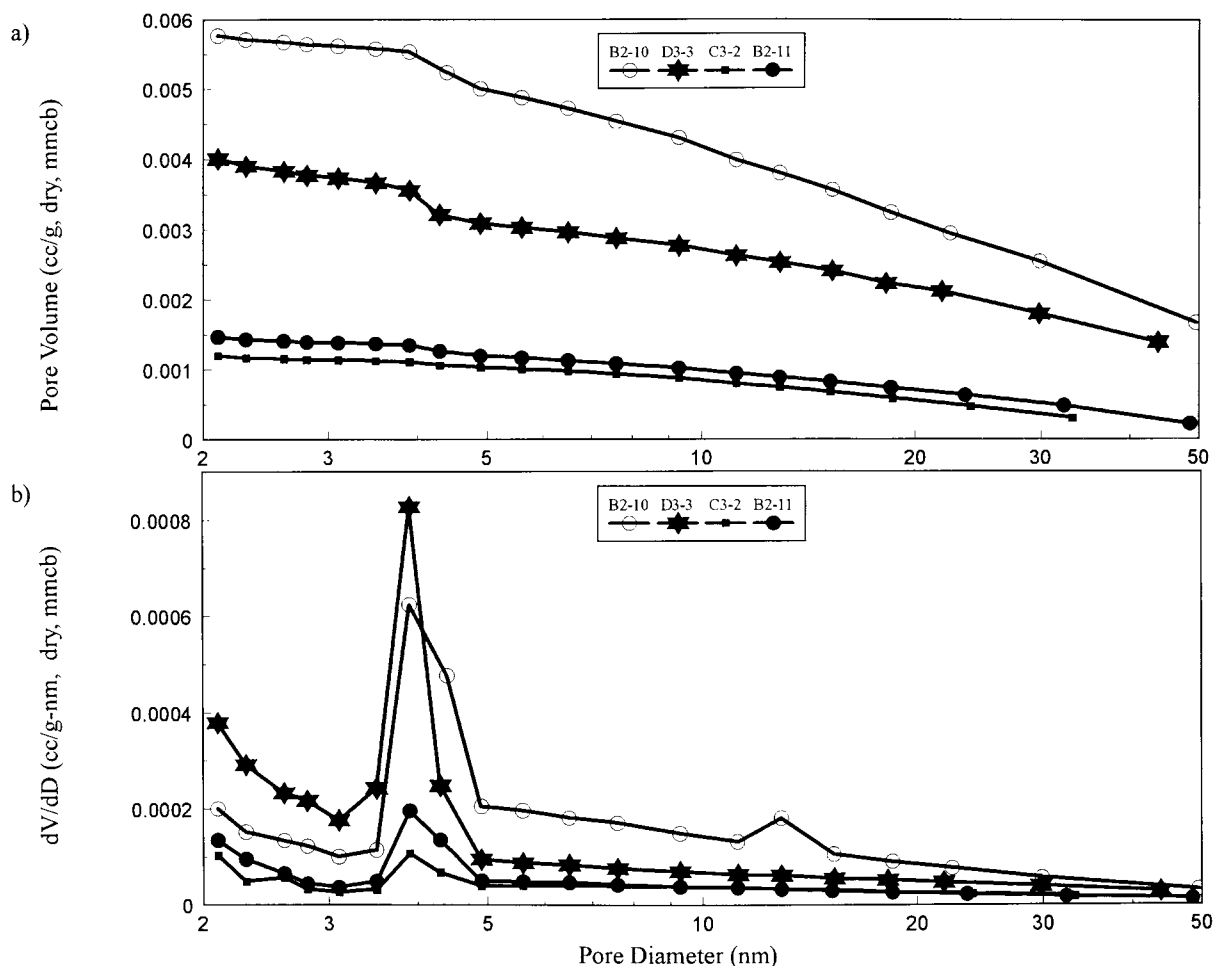
Fig. 3. Cumulative desorption pore volume plots (a) and pore size distributions (b) obtained from nitrogen isotherm.

Washburn equation to determine pore size distributions [21].

3. Results and discussion

3.1. Coal petrographic data

The selected Gates coals vary markedly in their maceral and ash contents, and therefore represent a wide range in composition (Table 1). The four coals represent three different lithotypes: bright (C3-2); banded bright (B2-11) and dull (B2-10 and D3-3). Two coals (C3-2 and B2-11) have high vitrinite (>50 vol%, mineral matter-free) and low ash (<20 wt.%) contents, whereas samples B2-10 and D3-3 have low vitrinite (<50%) and high ash (>20%) contents.

3.2. Low pressure carbon dioxide sorption isotherm data

Low-pressure carbon dioxide isotherms (273 K) (Fig. 1)

Table 3
Densities and total pore volumes of (-4 mesh) coals. Numbers in parenthesis indicate number analyses performed

Sample	Hg density (g/cm³, dry, mmcb)	Hg density (g/cm³, daf)[a]	He density (g/cm³,dry, mmcb)	He density (g/cm³, daf)	Total pore volume (cm³/g, dry, mmcb)[b]	Total pore volume (cm³/g, daf)[b]
C3-2	1.36 (1)	1.27	1.40 (3)	1.30	.021	.024
B2-11	1.28 (2)	1.26	1.35 (3)	1.33	.043	.045
D3-3	1.75 (2)	1.34	1.80 (3)	1.40	.016	.030
B2-10	1.74 (3)	1.51	1.81 (3)	1.59	.023	.032

[a] Assume ash density = 2.7 g/cc.

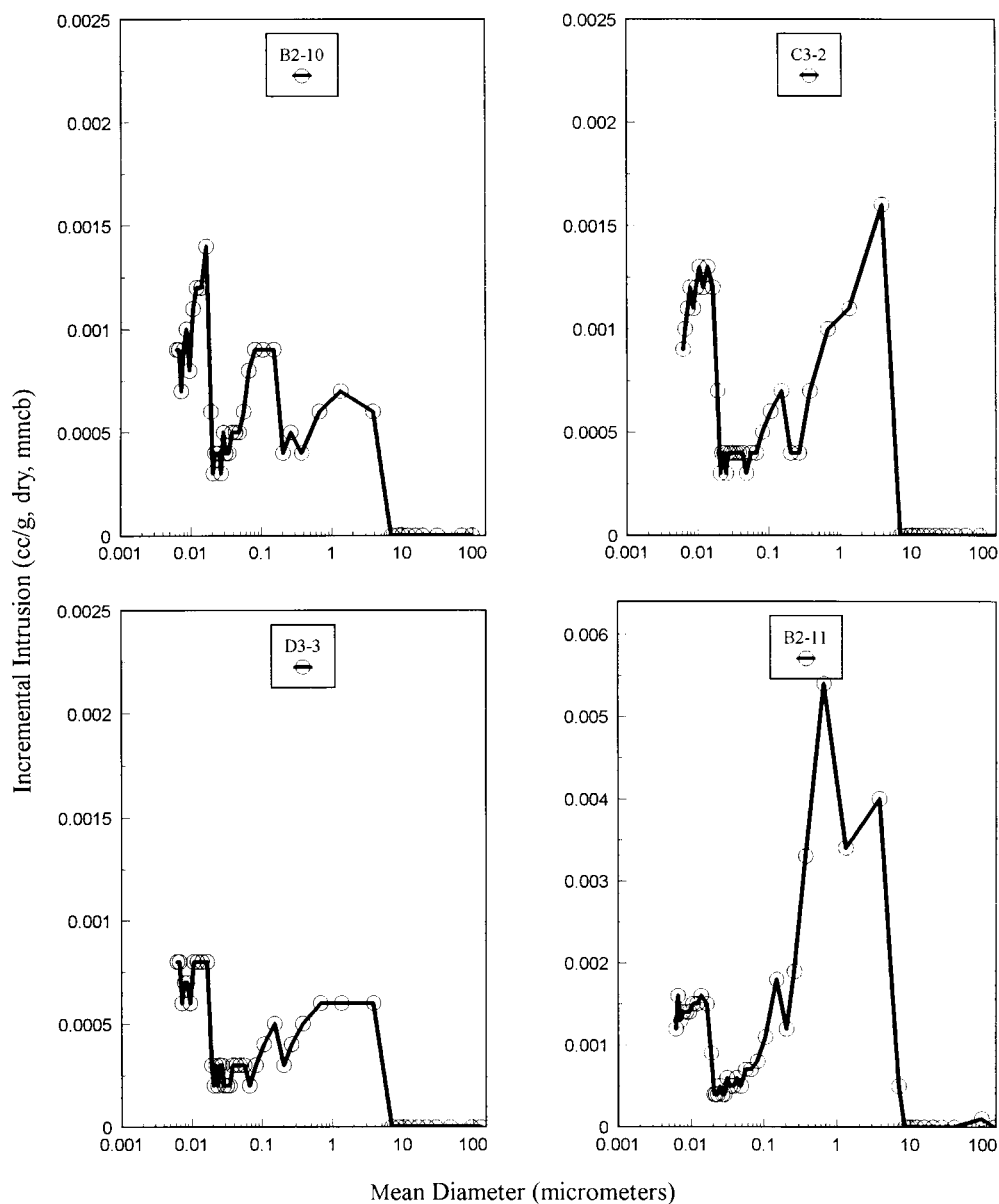[b] $V_T = (\frac{1}{\rho_{Hg}} - \frac{1}{\rho_{He}})$.

Fig. 4. Mercury incremental intrusion vs. pore diameter curves for -4 mesh splits. Note the scale change for sample B2-11.

demonstrate that the high vitrinite, low ash coals (C3-2 and B2-11) have higher adsorbed carbon dioxide volumes than the low vitrinite, high ash coals (D3-3 and B2-10) on a dry, mineral matter containing basis (mmcb). Carbon dioxide micropore volumes obtained for the -60 mesh coals, using the D–R equation, are given in Table 2. D–R micropore volumes obtained from -4 mesh splits of the coals are also given in Table 2. Close agreement between the values obtained for -60 and -4 mesh coals indicate that the splits are relatively homogeneous and that particle size has a negligible effect upon micropore volumes. The banded bright and bright coals B2-11 and C3-2 have a greater micropore volume (.057 cc/g, daf) than the dull coals D3-3 and B2-10 (.046 and.040 cc/g, respectively), which is consistent with previous studies [13,15]. Such results are

attributed to a greater amount of microporosity in vitrinite-rich samples.

3.3. Low pressure nitrogen sorption isotherm data

Low-pressure nitrogen (77 K) isotherms (Fig. 2) are Type II (C3-2, B2-11) or IV (B2-10, D3-3) according to the Brunauer, Deming, Deming and Teller classification [30]. The high ash, high inertinite coals display a greater amount of hysteresis than do the high vitrinite, low ash coals. Results are given here on a mineral-matter-containing basis (mmcb) as the contribution of entrained mineral matter to nitrogen adsorption is unknown. The hysteresis loop that terminates (desorption) at a relative pressure of ~0.45 is a Type H3, indicating slit-shaped pores [31]. The
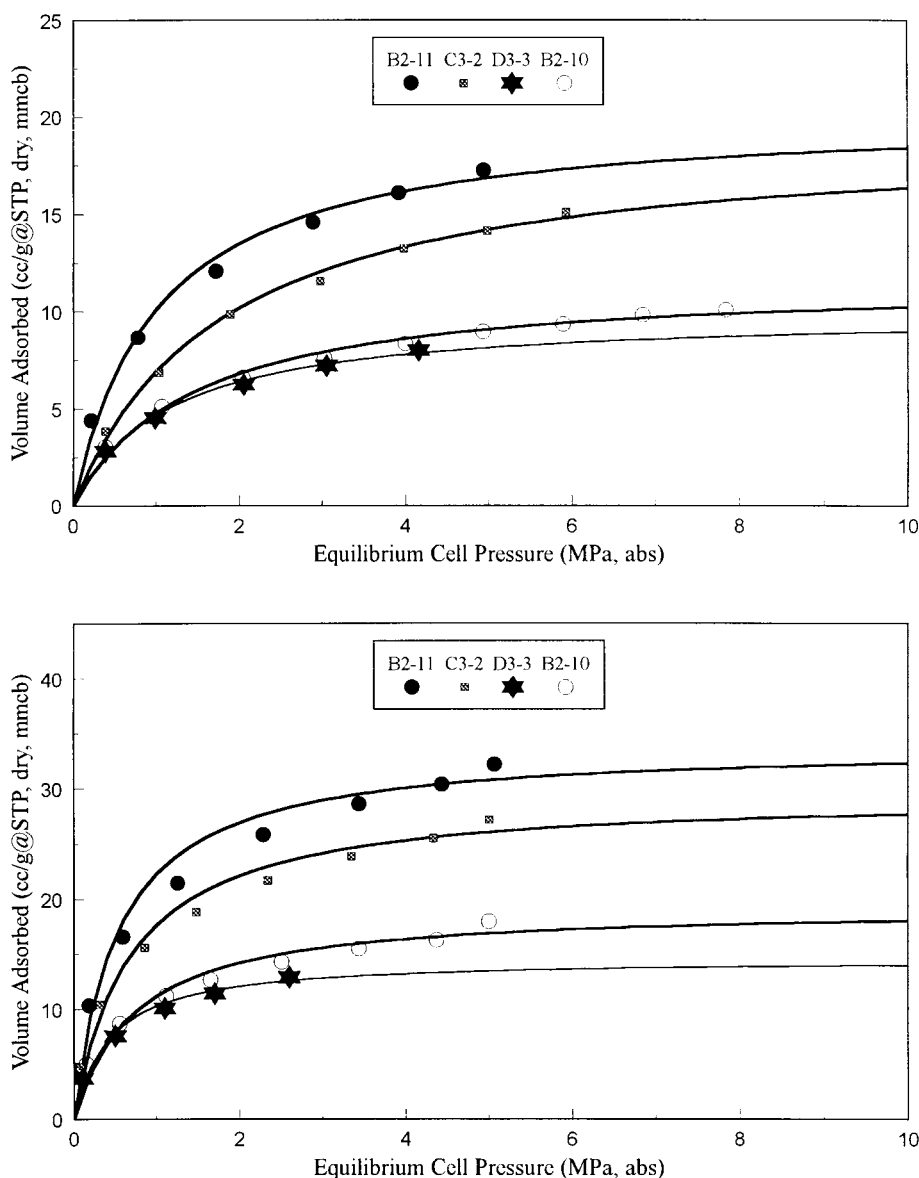
Fig. 5. High-pressure 303 K (a) methane and (b) carbon dioxide isotherms for dry -4 mesh splits. Lines are Langmuir fit to data.

lack of closure of the hysteresis loop below a relative pressure of 0.45 may be due to swelling of the coal during adsorption [21].

Nitrogen BET surface areas (Table 2) are larger for the dull coals (>2 m²/g) than for the bright and banded bright coals (<1 m²/g). Gan et al. [5] similarly obtained nitrogen surface areas that were less than 1 m²/g for some coals. Those authors [5] stated that nitrogen is probably not accessible to particulate minerals in the organic matrix of coal at the low temperatures. The dull coals have a greater amount of mesoporosity than the bright and banded bright coals, as evidenced by the cumulative pore volume plots (Fig. 3(a)) and BJH mesopore volumes (Table 2). All the samples have a pore volume distribution peak at around 4 nm (Fig. 3(b)). A peak in this size range may only indicate that finer pores are present and hence may be an artifact

[7,21]. Sample B2-10 has an additional (minor) peak at about 13 nm.

3.4. He and Hg porosimetry

Mercury and helium densities, and total pore volumes for all coals are given in Table 3. The total pore volumes of all coals are actually less than the D–R micropore volumes. This finding is not unusual; the data of Walker et al. [29] demonstrates that CO_2 micropore volumes (V_{CO_2}) are greater than the total pore volume for some coals. Unsworth et al. [7] found that V_{CO_2} for inertinite-rich ($>50\%$) coals are larger than the volume in pores <30 nm. Unsworth et al. [7] suggested that the discrepancy is due to preferential adsorption of CO_2 (perhaps on oxygen functionalities) causing some swelling to occur.
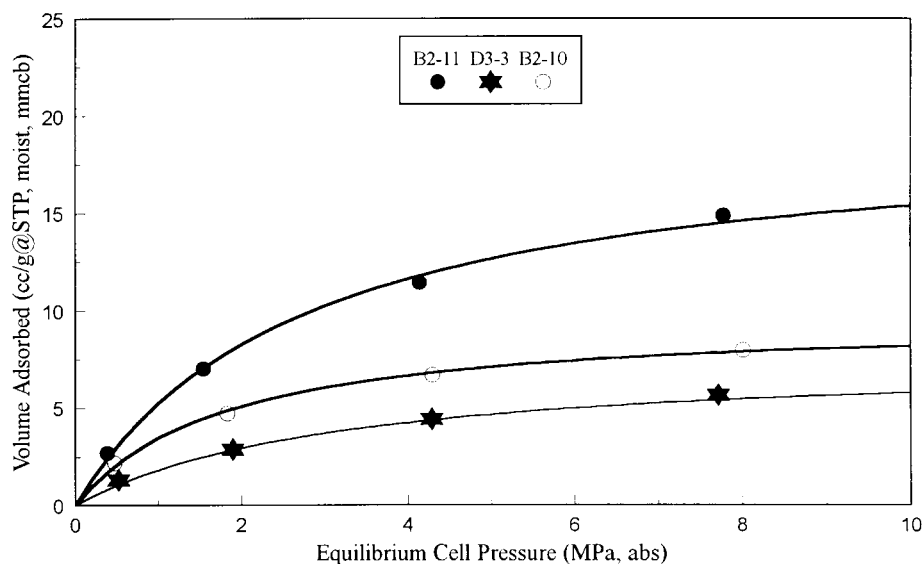
Fig. 6. High-pressure 303 K methane isotherms for moisture-equilibrated -4 mesh splits. Lines are Langmuir fit to data.

Owing to the highly compressible nature of coal, and the possibility of opening otherwise closed porosity at high-pressure, pore volume distributions obtained from mercury porosimetry must be viewed with caution [32]. This is especially true for pressures greater than 68 MPa (10 000 psi). However, qualitative information may be obtained about the pore structure.

All Gates samples are multimodal with respect to pore volume distribution (Fig. 4). Samples B2-11 and C3-2 have large peaks at around 1000 nm. Sample B2-11 appears to contain the greatest amount of macroporosity, possibly due to the large amounts of semifusinite in the sample.

The suite of coals chosen for the current study represents a broad range in pore structural characteristics. In particular, the high vitrinite, low ash coals have a greater percentage of microporosity than the low vitrinite, high ash coals. Conversely, the low vitrinite, high ash coals have a greater percentage of mesoporosity.

3.5. High-pressure adsorption isotherm data

High-pressure methane isotherms collected for dried (Fig. 5) and moisture equilibrated (Fig. 6) -4 mesh coals are essentially identical with the -60 mesh coal isotherms, indicating that equilibrium had been reached in the allotted time. The moisture-equilibrated -4 mesh C3-2 coal did not reach equilibrium in the allotted time and therefore this data is not used.

Considerably more carbon dioxide than methane is adsorbed on to the dry coals (Fig. 5), which is consistent with previous studies [33–36]. Carbon dioxide isotherms have a slight inflection at high-pressure, possibly a result of multilayer adsorption [36]. Significant enhancement of carbon dioxide adsorption at high-pressures would have

important implications for the injection of carbon dioxide into coal gas reservoirs at high-pressures [36].

Although the Langmuir equation (1) was fit to the data in Fig. 5, a better fit to the data was obtained by using the D–A equation (2) (Fig. 7). This is particularly true for the carbon dioxide data, where the average relative error [28] may be as large as 13% for the Langmuir equation but is generally less than 2% for the D–A equation.

The high vitrinite/low ash coals have a higher adsorption capacity than the low vitrinite/high ash coals for both methane and carbon dioxide (Table 4, Fig. 5). If the results are plotted on a dry, ash-free basis (Fig. 8), the high vitrinite coals still adsorb more methane and carbon dioxide, but there is less separation than for isotherms plotted without correcting for ash content. Previous studies [15] have shown that, although gas adsorption tends to increase with an increase in vitrinite content, the highest adsorbing coals do not have the highest vitrinite content but have a mixture of vitrinite and inertinite. This appears to be the case for the current suite of samples; sample B2-11 has the highest adsorption capacity, but does not have the highest vitrinite content. As suggested by Lamberson and Bustin [15], semifusinite may also contribute substantially to the adsorption capacity of some coals.

3.6. Towards a pore structural model for sorption rate analysis

Some general observations may be made regarding the pore structure of different lithotypes despite the difficulties of obtaining a quantitative evaluation of the pore volume distribution of coals from gas adsorption/mercury porosimetry. All the studied coals are multimodal with respect to pore volume distribution, but have varying proportions of micro-, meso-, and macroporosity. In particular, bright and banded
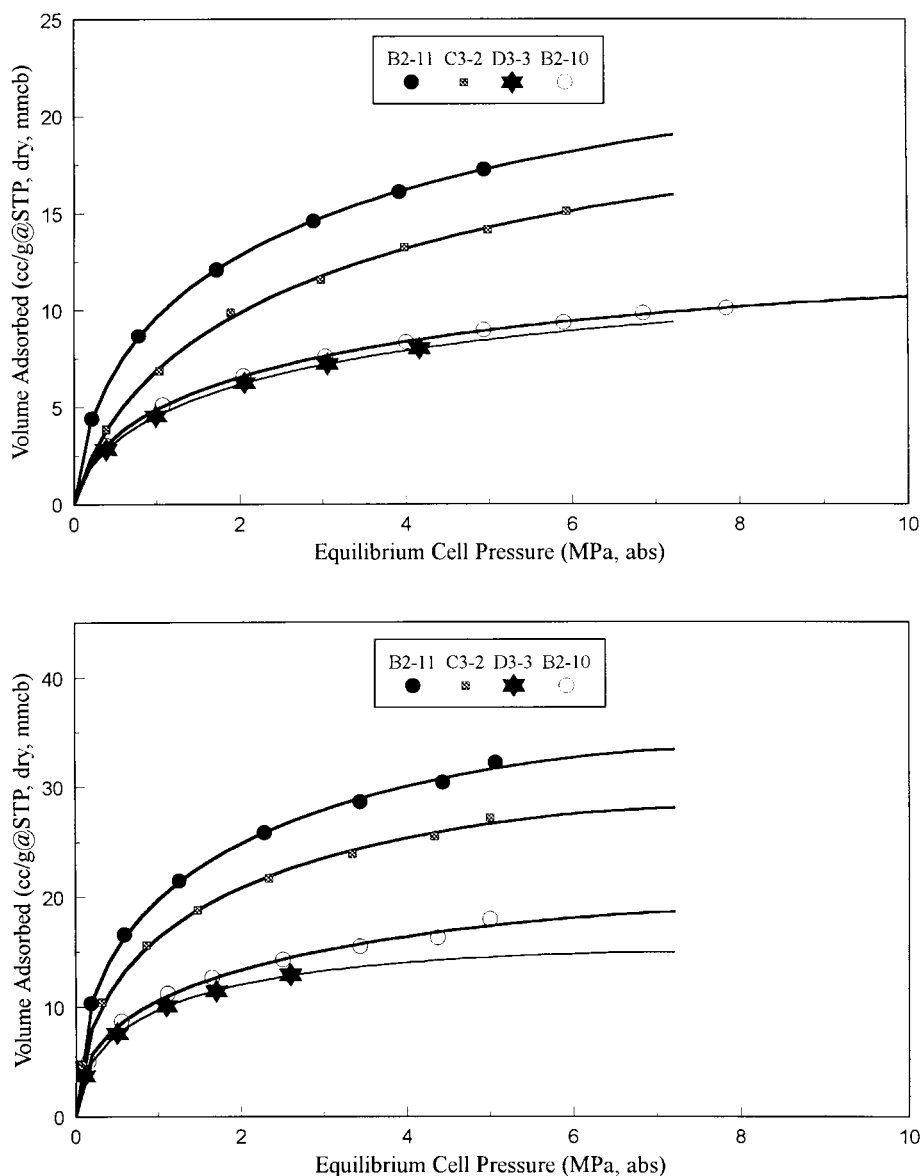
Fig. 7. High-pressure 303 K (a) methane and (b) carbon dioxide isotherms for dry -4 mesh splits. Lines are D–A fit to data.

bright coals have a greater micropore volume than dull coals of equivalent rank, whereas dull coals have a greater proportion of mesopores, as evidenced by nitrogen isotherm hysteresis loops, and an estimation of mesopore volume from BJH theory. Mercury porosimetry indicates that although all coals have large pore volume distribution peaks in the macropore range, one coal, B2-11, has a much greater amount of macroporosity.

Table 4
Langmuir parameters for high-pressure methane and carbon dioxide isotherm data. Langmuir volumes reported on a moist, mineral matter-containing basis

Sample	CH_4 on dry coal[a]		CH_4 on wet coal[b]		CO_2 on dry coal[b]	
	V_L (cm^3/g, STP)	P_L (MPa)	V_L (cm^3/g, STP)	P_L (MPa)	V_L (cm^3/g, STP)	P_L (MPa)
C3-2	18.4 (3)	1.4 (3)	–	–	29.6 (1)	0.7 (1)
B2-11	20.5 (3)	1.0 (3)	19.7 (1)	2.7 (1)	34.0 (1)	0.5 (1)
D3-3	9.1 (2)	1.0 (2)	7.6 (1)	2.9 (1)	14.6 (1)	0.4 (1)
B2-10	11.1 (3)	1.2 (3)	9.7 (1)	1.8 (1)	19.4 (1)	0.7 (1)

[a] First six points on isotherm (up to 5 MPa) were used in Langmuir regression for comparison.
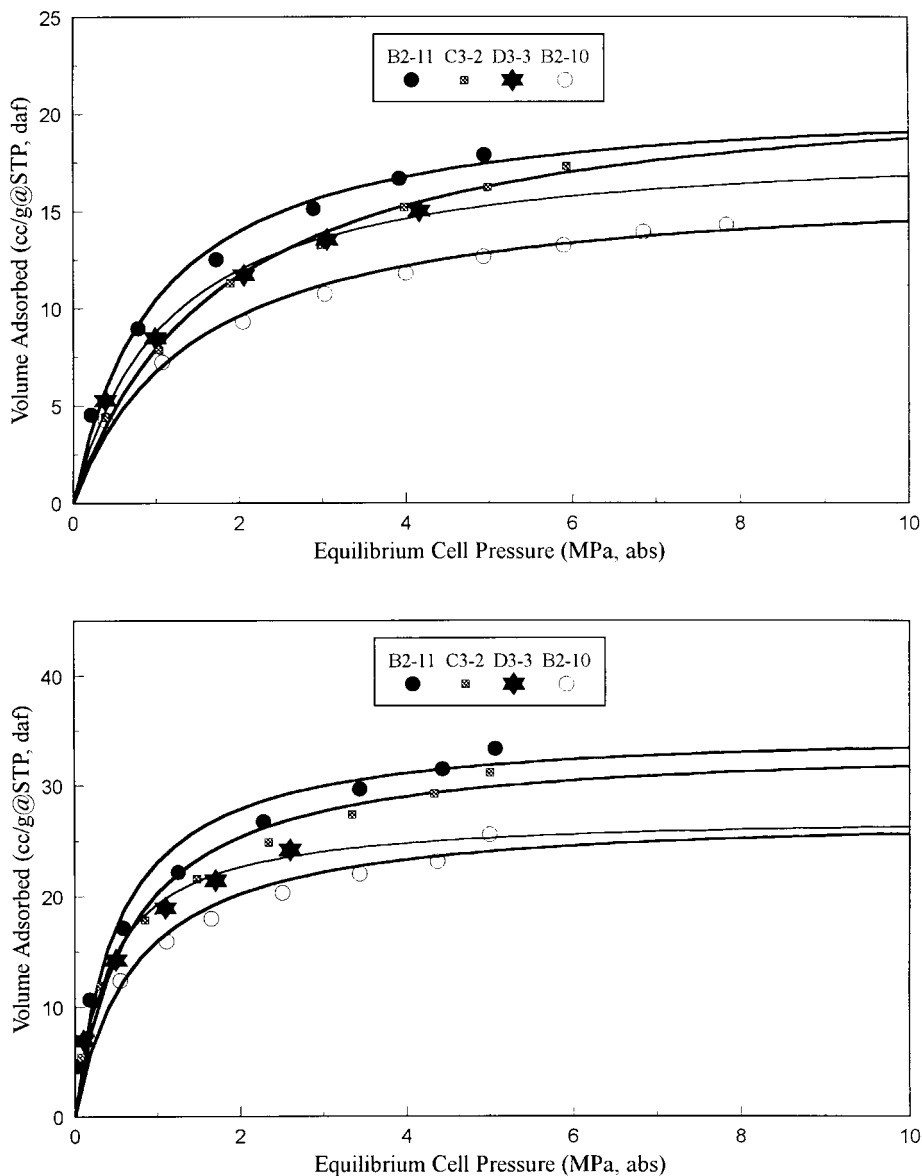[b] All points on isotherm used in Langmuir regression.

Fig. 8. High-pressure 303 K (a) methane and (b) carbon dioxide isotherms for dry -4 mesh splits. Lines are Langmuir fit to data.

Although the findings of the current study are, in part, consistent with the Unsworth et al. [7] study for low rank bituminous coals, who found that inertinite-rich coals generally have a higher mesoporosity than vitrinite-rich coals, it is probably not sufficient to state that vitrinite-rich coals have less macroporosity than inertinite-rich coal. Sample B2-11, which has >50% vitrinite (mmf), contradicts this trend. A number of factors including maceral and mineral composition and abundance affect pore volume distribution and the pore structure has been shown to be a function of rank [5].

The pore volume distributions may be used to predict the gas adsorption capacity of coal. Langmuir volumes for high-pressure methane adsorption on dry and moisture-equilibrated coal as well as carbon dioxide on dry coal are plotted against micropore volume (mmcb) in Fig. 9. For each

system, a linear increase in Langmuir volume, which is an estimate of total gas capacity, with micropore volume is observed, suggesting that micropore volume is the main control upon gas adsorption. Previous studies [25,38] have shown a similar trend for methane-coal systems, but it is obvious that micropore volume is also a control upon high-pressure carbon dioxide adsorption. Mesoporosity does not appear to have an important effect upon methane total gas capacity, although dull coals have a greater proportion of mesoporosity than bright and banded bright coals in this coal suite. The occurrence of an inflection in the high-pressure carbon dioxide isotherms, which could be attributed to the formation of multilayers in larger (meso)pores, may indicate that adsorption in mesoporosity is significant for carbon dioxide.

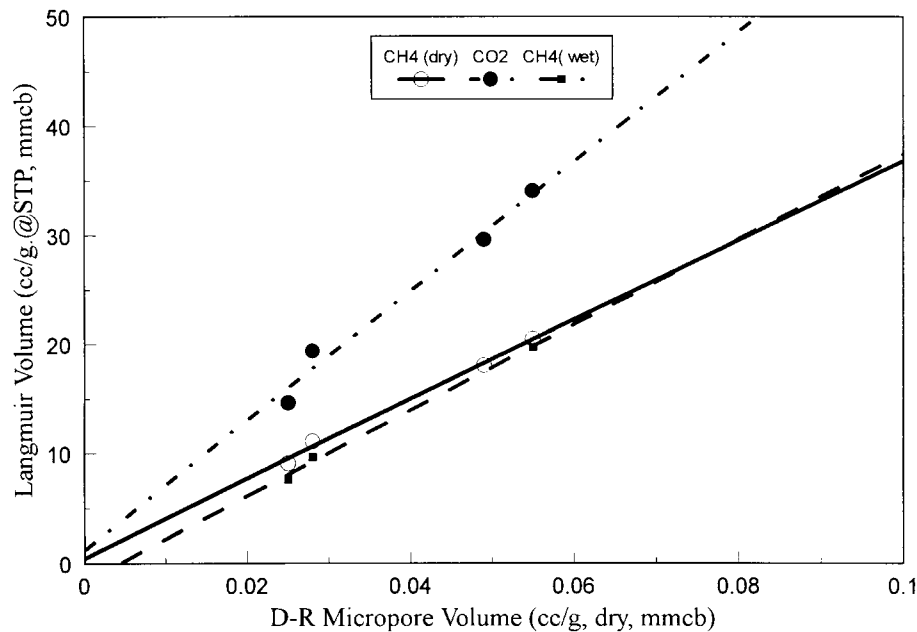A comprehensive coal matrix gas transport model must

Fig. 9. Langmuir volume vs. D–R micropore volume (mmcb).

account for many of the observations described earlier. Coal pore volume distribution, which varies with composition and rank, is typically multimodal, and therefore matrix transport models must describe transport in several pore systems. Equilibrium gas adsorption isotherms are

for the above observations and is an extension of previous models, is developed in Part 2.

4. Conclusions

A variety of conventional adsorption/porosimetry analyses have been applied to four bituminous coal samples in order to determine the coal pore volume distribution and gas adsorption capacities. Pore volume distributions and gas adsorption capacities may reasonably be assumed to have an important effect upon gas transport properties of coal. Each analytical technique has some limitation in terms of either the accessibility of the adsorbate to the internal coal structure, complex interaction of the adsorbate with the coal, range of application, or physical distortion of the coal structure during analysis. In addition, problems with data interpretation exist [37]. The combination of gas adsorption/porosimetry, however, is useful in characterizing the properties of coal which affect the gas adsorption and adsorption

rate properties of coal, and hence the ultimate gas capacity and transport properties. The usefulness of combined analyses in terms of explaining the adsorption rate behavior of coals of varying lithotype composition and hence pore structure, will become clear in the paper that follows (Part 2).

The following conclusions have been made regarding the pore volume distributions and adsorption properties of the four coal lithotypes utilized in this study:

(1) Bright and banded bright (high-vitrinite, low ash) coals have a greater micropore volume than dull (low vitrinite-high ash) bituminous coals of equivalent rank, as determined from low-pressure carbon dioxide adsorption. This finding is consistent with previous laboratory investigations.

(2) Dull coals have a greater amount of mesoporosity than bright coals as assessed from nitrogen adsorption/desorption analysis. Nitrogen adsorption/desorption isotherms indicate a slit-shaped mesopore shape.

(3) Mercury porosimetry shows that the coals have a multimodal pore volume distribution. The banded bright coal (B2-11) has a relatively large peak in the macropore range, possibly due to high amounts of semifusinite in the sample.

(4) High-pressure methane and carbon dioxide isotherms illustrate that bright and banded bright coals adsorb more gas than dull coals. Correction of the isotherms to a dry-ash free basis yields the same general relationship, indicating that maceral type is a control upon gas adsorption, but there is less of a discrepancy between coals. The Dubinin–Astakhov equation provides a better fit to the isotherm data than the conventionally used Langmuir equation.

High-pressure methane and carbon dioxide Langmuir

volumes, used as an estimate of total gas capacity, are linearly correlated with Dubinin–Radushkevich micropore volumes, obtained from low-pressure carbon dioxide adsorption. This finding illustrates that micropore volume is the primary control upon gas adsorption in the Gates coals.

Acknowledgements

References

[1] Smith DM, Williams FL. Soc Petrol Engng J 1984;24:529.
[2] Smith DM, Williams FL. Coal science and chemistry. Amsterdam: Elsevier, 1987. p. 381–403.
[3] Olague NE, Smith DM. Fuel 1989;51:1381.
[4] Beamish BB, Crosdale PJ. Proceedings of the International Symposium cum Workshop on Management and Control of High Gas Emission and Outbursts. Wollongong, 20–24 March, 1995. p. 353–61.
[5] Gan H, Nandi SP, Walker Jr. PL. Fuel 1972;51:272.
[6] Parkash S, Chakrabartty SK. Int J Coal Geol 1986;6:55.
[7] Unsworth JF, Fowler CS, Jones LF. Fuel 1989;68:18.
[8] Faiz MM, Aziz NI, Hutton AC, Jones BG. Proceedings, Symposium on Coalbed Methane Research and Development in Australia. Townsville, Queensland, 1992. p. 9–20.
[9] International Union of Pure and Applied Chemistry, Pure Appl Chem, 1994;66:1739.
[10] Toda Y, Hatami M, Toyoda S, Yoshida Y, Honda H. Fuel 1971;50:187.
[11] Debelak KA, Schrodt JT. Fuel 1979;58:732.
[12] Amarasekera G, Scarlett MJ, Mainwaring DE. Fuel 1995;74:115.
[13] Clarkson CR, Bustin RM. Fuel 1996;75:1483.
[14] Anderson RB, Bayer J, Hofer LJE. Fuel 1965;44:443.
[15] Lamberson MN, Bustin RM. AAPG Bull 1993;77:2062.
[16] Levine JR, Johnson P, Beamish BB. Proceedings of the 1993 International Coalbed Methane Symposium. Tuscaloosa, May 17–21, 1993. p. 187–95.
[17] Bustin RM, Clarkson C, Levy J. Proceedings of the 29th Newcastle Symposium, Advances in the Study of the Sydney Basin, University of Newcastle, 1995. p. 22–8.
[18] Ettinger I, Eremin I, Zimakov B, Yanovshaya M. Fuel 1966;45:267.
[19] Bustin RM, Cameron AR, Grieve DA, Kalkreuth WD. Coal petrology: its principals, methods and applications. 2. Geological association of Canada short course notes, 3, 1985.
[20] Perch M. In: Elliot MA, editor. Chemistry of coal utilization, New York: Wiley, 1981. pp. 943. Second supplementary volume.
[21] Gregg SJ, Sing KSW. Adsorption surface area and porosity. 2. New York: Academic Press, 1982.
[22] Brunauer S, Emmett PH, Teller E. J Am Chem Soc 1938;62:1723.
[23] Barrett EP, Joyner LG, Halenda PP. J Am Chem Soc 1951;73:373.
[24] Mavor MJ, Owen LB, Pratt TJ. Paper SPE 20728, presented at the 65th Annual Technical Conference of the Society of Petroleum Engineers. New Orleans, Louisiana, September 23–26, 1990. p. 1–14.
[25] Levy JH, Day SJ, Killingley JS. Fuel 1997;74:1.
[26] Levy JH, Killingley JS, Day SJ. Proceedings of the Symposium on Coalbed Methane Research and Development in Australia, vol. 4, 1992. p. 1–8.
[27] Langmuir I. J Am Chem Soc 1918;40:1361.
[28] Clarkson CR, Bustin RM, Levy JH. Carbon 1997;35:1689.
[29] Walker Jr. PL, Verma SK, Rivera-Utrilla J, Davis A. Fuel 1988;67:1615.
[30] Brunauer S, Deming LS, Deming WS, Teller E. J Am Chem Soc 1940;62:1723.
[31] Sing KSW, Everett DH, Haul RAW, Moscou L, Pierotti RA, Rouquerol J, Siemieniewska T. Pure Appl Chem 1985;57:603.
[32] Mahajan OP, Walker Jr. PL. In: Karr Jr. C, editor. Analytical methods for coal and coal products, New York: Academic Press, 1978. pp. 150.
[33] Stevenson MD, Pinczewski WV, Somers ML, Bagio SE. SPE Paper 23026, presented at the SPE Asia-Pacific Conference. Perth, Western Australia, November 4–7, 1991. p. 41–55.
[34] Greaves KH, Owen LB, McLennan JD. Proceedings of the 1993 International Coalbed Methane Symposium. Tuscaloosa, May 17–21, 1993. p. 151–60.
[35] Harpalani S, Pariti UM. Proceedings of the 1993 International Coalbed Methane Symposium. Tuscaloosa, May 17–21, 1993. p. 151–60.
[36] Hall FE, Zhou C, Gasem KAM, Robinson RL, Jr., Yee D. SPE Paper 29194, presented at the Eastern Regional Conference and Exhibition. Charleston, WV, November 8–10, 1994. p. 329–43.
[37] Glaves CL, Davis PJ, Gallegos DP, Smith DM. Energy and Fuels 1988;2:662.
[38] Smith DM, Williams FL. Coal science and chemistry. Amsterdam: Elsevier, 1987. p. 381.